JOURNAL OF MATERIALS SCIENCE 24 (1989) 1015–1020

# Processing to optimize the strength of heavily drawn Cu–Nb alloys

J. D. VERHOEVEN, W. A. SPITZIG, F. A. SCHMIDT, P. D. KROTZ, E. D. GIBSON
*Ames Laboratory and Department of Materials Science, and Engineering, Iowa State University, Ames, Iowa 50011, USA*

Heavily drawn Cu–Nb alloys display quite high ultimate tensile strengths. A modification to the consumable arc-casting technique used to prepare these alloys is shown to decrease the as-cast niobium dendrite diameter, $t_0$, and also increase strength. Evaluation of strength, niobium filament spacing and thickness data show that strength varies with as-cast niobium dendrite size as somewhere between $t_0^{-0.36}$ to $t_0^{-0.50}$. Splat-cooling techniques demonstrate that minimum niobium dendrite sizes as small as 0.22 $\mu$m are possible. These sizes are over a factor of 10 smaller than has been achieved by consumable arc casting, and it is therefore suggested that processing rapidly solidified powders of Cu–Nb alloys should have significant advantages for preparing high-strength heavily drawn Cu–Nb alloys.

## 1. Introduction

It was first demonstrated by Bevk *et al.* [1] that if a cast Cu–18 wt % Nb alloy was drawn to very large reductions, quite high tensile strengths, over 2000 MPa, could be achieved. Such cast alloys consist of arrays of nearly pure niobium dendrites in a nearly pure copper matrix. Both phases are sufficiently ductile that extensive drawing may be done without need for annealing. The extensive drawing causes the niobium dendrite branches to axially align and the final wire is essentially a metal/metal-matrix composite of aligned niobium fibres in a copper matrix. Because of the manner in which the composite structure forms, these materials are often termed *in situ* composites, but they will be called heavily drawn composites here because that name seems more descriptive.

Based primarily upon a study of the resistivity of such Cu–Nb composites, Karasek and Bevk [2, 3] concluded that these materials contained extremely high dislocation densities ($10^{13}\,cm^{-2}$) when drawn to the high strength levels. Funkenbusch and co-workers [4, 5] have developed a theory for the strengthening of these alloys which attributes the high strength to the high dislocation densities. Karasek, and Bevk [2] report that such high dislocation densities are consistent with the TEM data of [1], but a recent TEM study by Pelton *et al.* [6] reports maximum dislocation densities of only $10^{10}\,cm^{-2}$. Another study [7] on heavily rolled sheet material found that the maximum dislocation density never exceeded $10^{11}\,cm^{-2}$.

Recent work by Spitzig *et al.* [8] shows that the ultimate tensile strength, $\sigma$, correlates with the niobium filament spacing, $\lambda$, following a Hall–Petch relationship

$$\sigma = 65 + 1000\lambda^{1/2} \quad (1)$$

where $\lambda$ is in $\mu$m and $\sigma$ in MPa. It was also found that the spacing reduced with draw ratio, $\eta$, as

$$\lambda = \lambda_0 e^{-0.36\eta} \quad (2)$$

where $\lambda_0$ is the mean spacing measured on the as-cast alloy and $\eta = \ln(A_0/A)$, where $A_0/A$ = initial billet area/final wire area. Combining Equations 1 and 2 the following relation is found

$$\sigma = 65 + 1000\, e^{0.18\eta}/\lambda_0^{1/2} \quad (3)$$

Spitzig *et al.* [8] attribute the large strengthening produced in these materials to the difficulty in transmitting plastic flow across the Nb/Cu filamentary interfaces. More recent data show that additional strengthening mechanisms must also be important because the strength level at constant $\lambda$ on material of constant volume fraction of niobium are different for sheet compared to wire [9] and for wire having different initial dendrite sizes [10].

Irrespective of the strengthening mechanisms, the data of Spitzig *et al.* [8] show that to optimize strength one needs to reduce the as-cast niobium dendrite spacing, $\lambda_0$. It is sometimes more convenient to characterize the microstructure with the thickness of the dendrite diameter, $t_0$, rather than with spacing. For the study of Spitzig *et al.*, $\lambda_0 = 24.5\,\mu m$ and $t_0 = 6.2\,\mu m$. Taking the ratio of $\lambda/t$ constant for castings of different $\lambda_0$, but the same volume fraction of niobium, Equation 3 becomes

$$\sigma = 65 + 503\, e^{0.18\eta}/t_0^{1/2} \quad (4)$$

The major attractive feature of these highly drawn Cu–Nb alloys is their combination of high strength with high electrical and thermal conductivity. For comparison, consider the highest strength commercial copper alloy, Cu–Be, which at a tensile strength of 1600 MPa ($230 \times 10^3$ psi) has an electrical conductivity of 25% IACS. A recent study [11] on heavily drawn Cu–18 wt % Nb alloys demonstrated

0022–2461/89 $03.00 + .12 

an electrical conductivity of 66.6% IACS (International Annealed Copper Standard) at a tensile strength of 1450 MPa ($210 \times 10^3$ psi) in 1.1 mm diameter wire. This comparison shows that the heavily drawn Cu–Nb alloys display an improvement in electrical conductivity by a factor of 2 or more over Cu–Be at strength levels of around 1400 MPa ($203 \times 10^3$ psi). However, a major practical problem in producing commercial sizes of heavily drawn wire or sheet is the very large mechanical reductions required to achieve the increased strength. This may be demonstrated by evaluating the initial as-cast billet diameter that would be required to produce 3 mm (1/8 in.) diameter wire having a tensile strength of 1400 MPa, if the billet were reduced directly to wire. The study of Spitzig *et al.* utilized a 6.35 cm (2.5 in.) billet prepared by consumable arc casting and the average dendrite diameter was 6.2 $\mu$m. If this same dendrite diameter could be maintained in larger billets, Equation 4 predicts a drawing ratio of $\eta = 10.5$ is required to achieve 1400 MPa, which means the initial billet diameter would need to be 57 cm (22 in.). Even if the dendrite diameter could be held at 6.2 $\mu$m, such large billet diameters are not practical and it is clear that methods for reducing $t_0$ in the cast alloy are highly desirable. In this paper we describe experiments directed at achieving reduced values of $t_0$.

## 2. Experimental techniques

The Cu–19 wt % Nb ingot used in the study of Spitzig *et al.* [8] will be referred to as ingot A. This as-cast ingot had a diameter of 6.35 cm and it was machined down to a 6.1 cm diameter prior to mechanical reduction to wire. It was prepared by a consumable arc casting technique which has been described in general elsewhere [12]. The electrode was made by cutting longitudinal slots in a 3.5 cm diameter by 91 cm long solid copper rod and inserting 0.3 cm × 2.5 cm × 91 cm strips of niobium in the slots. This composite electrode was arc melted under a pressure of 0.75 atm argon into a water-cooled copper can using 1800 to 2000 A at 28 to 30 V. To avoid the danger of burning through the copper mould, a graphite liner was fitted inside it having an inside diameter of 6.35 cm and a wall thickness of 1.27 cm. The inside surface of the graphite was plasma sprayed with $Y_2O_3$-stabilized $ZrO_2$ to minimize carbon contamination of the melt. Metallographic examination of sections of the cast ingot revealed a fairly uniform distribution of niobium dendrites across the entire diameter of the ingot. The average dendrite size was measured as 6.2 $\pm$ 1.0 $\mu$m using standard stereology techniques on an optical microscope.

In the present study the consumable arc melting process was modified to eliminate the graphite liner and this change proved effective at reducing $t_0$. In order to reduce the possibility of a burn-through at the copper mould wall, a new mould was fabricated. The inside diameter was kept at 7.5 cm (3 in.) but the wall thickness was increased from 1.2 cm to 5.7 cm. An electrode identical to that used for ingot A was arc melted directly into this mould which was water cooled on its outside surface. The current/voltage conditions were 2000 A/28 V and no trouble was encountered with melting of the mould wall, which was thought to be a possibility because of the nearly equal thermal conductivity between the mould material and the Cu–19 wt % Nb alloy. The solidified ingot was found to have a few isolated regions where 2 to 3 mm globs of nearly pure dendritic niobium had formed. To overcome this problem the ingot was cut longitudinally into four sections which were then pressed to a more round shape and welded end-to-end to form a new electrode. A second melt was made with this new electrode and metallographic examination of this ingot revealed that the globular niobium regions had been eliminated. It was found, however, that although the niobium dendrite sizes were uniform in the interior of the ingot, they were significantly finer in the outer $\sim$ 6 mm rim of the ingot. Therefore the double melted ingot (ingot B) was machined down from 7.5 to 6.1 cm prior to mechanical reduction to wire form. The 6.1 cm diameter was identical to that employed for ingot A and the reduction schedule for producing wire, rod rolling followed by wire drawing, was also identical.

TABLE I The mean niobium dendrite size measured at five radial locations in ingot B. $R$ = ingot radius = 3.81 cm (1.5 in.)

| Radial position | Mean niobium dendrite size ($\mu$m) |
|---|---|
| $r$ = 0 (centre) | 3.9 |
| $r$ = 1/4$R$ | 3.3 |
| $r$ = 1/2$R$ | 4.6 |
| $r$ = 3/4$R$ | 3.4 |
| $r$ = outer 6 mm rim | 1.8 |

A second type of experiment was performed to evaluate the minimum size of dendrites which might be achieved by rapid solidification. A small piece of ingot A was held above a water-cooled copper hearth under 0.75 atm argon pressure. The vertical surface of the ingot was melted by striking an arc against it with a tungsten electrode. This caused molten drops of the alloy to free-fall on to the surface of the water-cooled hearth. The molten drops formed splats of about 2 cm diameter which were thinner at their central regions, 0.5 mm, and fattened out to small radially protruding droplets up to 1 mm thick. These splats were deep etched and examined in the SEM to evaluate the $t_0$ values of the niobium dendrites which formed.

## 3. Experimental results

A transverse section of ingot B, located adjacent to the central portion of the ingot reduced to wire, was examined metallographically to evaluate dendrite size. Ten or more SEM photos were taken on the deep-etched section at the five radial positions shown in Table I. A size distribution plot was then made for over 100 dendrite arms at each radial position and the mean values at the five positions are given in Table I. The dendrite size in the outer rim is clearly smaller than in the central region. The dendrite size in the central region appeared to the eye to be fairly uniform and the data of Table I indicate an average size of $t_0 = 3.8\,\mu$m with a standard deviation of $\pm 0.8\,\mu$m.

After the ingot had been mechanically reduced

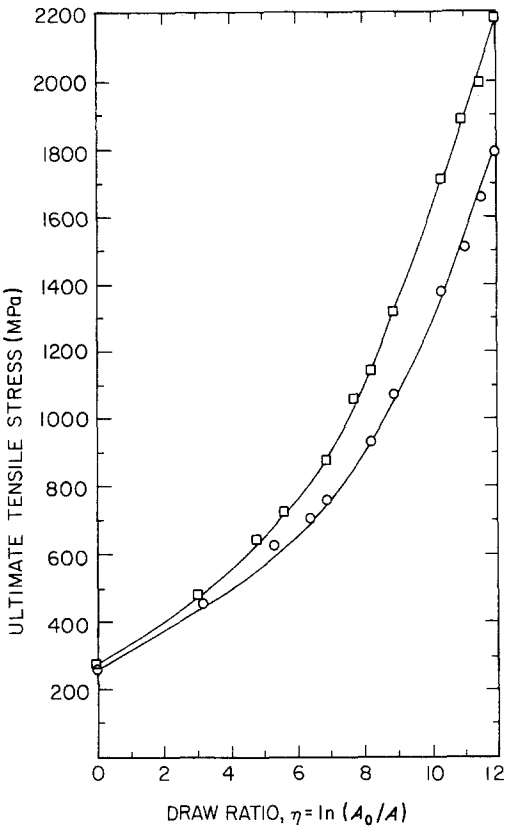


*Figure 1* Effect of draw ratio on the ultimate tensile stress of Cu–19 wt % Nb composites for two initial dendrite diameters: (□) $t_0 = 3.8\,\mu$m, (○) $t_0 = 6.2\,\mu$m.

to wire of various diameters down to a minimum diameter of 0.16 mm ($\eta = 11.9$), both the ultimate tensile strengths and the niobium filament spacings were determined. These data have been presented in more

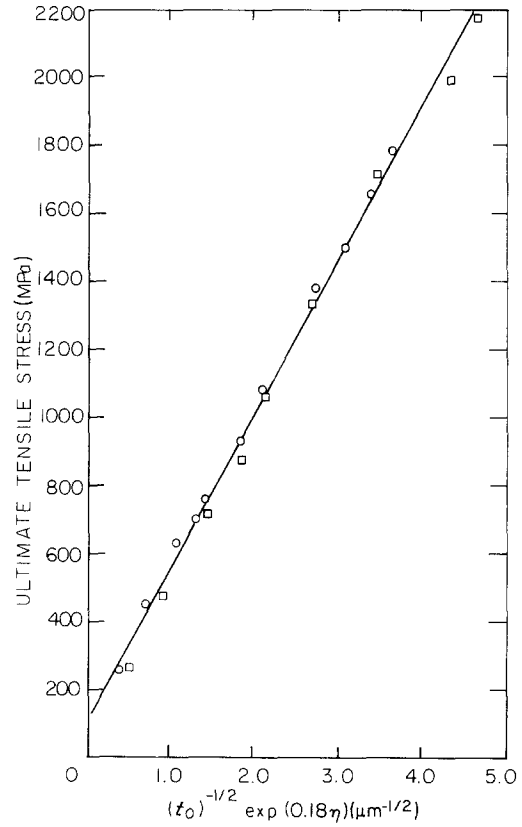


*Figure 2* Ultimate tensile stress dependence on the initial niobium dendrite size and the draw ratio ($\eta$) of Cu–19 wt % Nb composites. (□) $t_0 = 3.8\,\mu$m, (○) $t_0 = 6.2\,\mu$m.

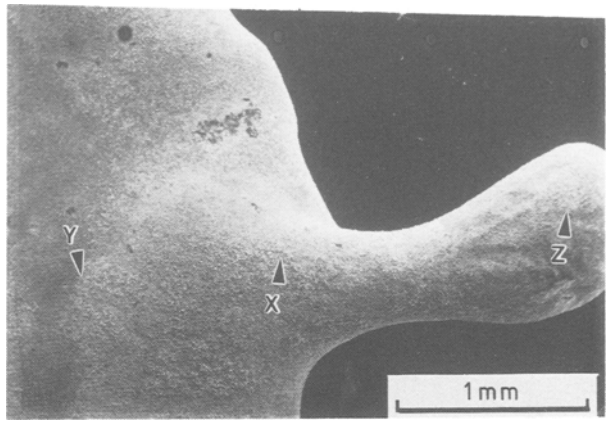


*Figure 3* Edge of Cu–19 wt % Nb splat.

detail elsewhere [13] and the principal findings are presented in Figs 1 and 2. It may be seen from Fig. 1 that, as expected, the smaller initial dendrite size obtained for ingot B has produced a significant increase in strength. The plot of Fig. 2 illustrates that the data are well correlated by an equation having the same form as Equation 3, which had been predicted from the data of ingot A only. The data from both ingots A and B shown in Fig. 2 give the following correlation

$$\sigma = 82 + 459\, e^{0.18\eta}/t_0^{1/2} \qquad (5)$$

Fig. 3 is a top view of one of the splats which formed when a drop of the molten Cu–19 wt % Nb alloy struck the water-cooled copper hearth. The thickness at the centre of this section, Y in Fig. 3, measured 0.5 mm, whereas the protruding finger at Z measured 0.8 mm. The sample was deep etched to remove the copper matrix and Figs 4 and 5 show the microstructures found at Y and X. The niobium microstructure consists of a mixture of well-formed dendrites and small spherical particles at both locations. At location Z, which had the lowest cooling rate, the spherical particles were absent and niobium dendrites coarser than at Y and X were observed. An average niobium dendrite arm size was evaluated by measuring 28 side arms in Fig. 3 and found to be $t_0 = 0.22 \pm 0.03\,\mu$m.

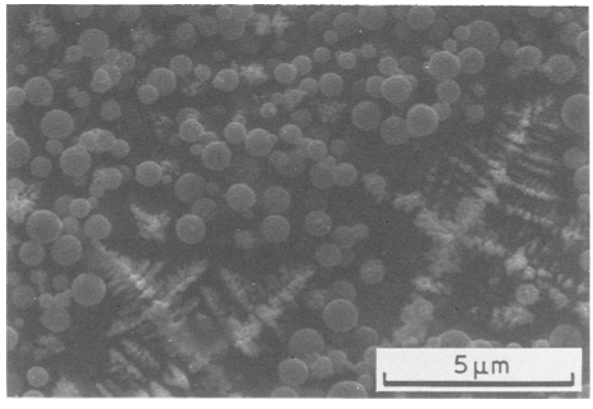


*Figure 4* Niobium microstructure after deep etching copper away. Location is point Y on Fig. 3.

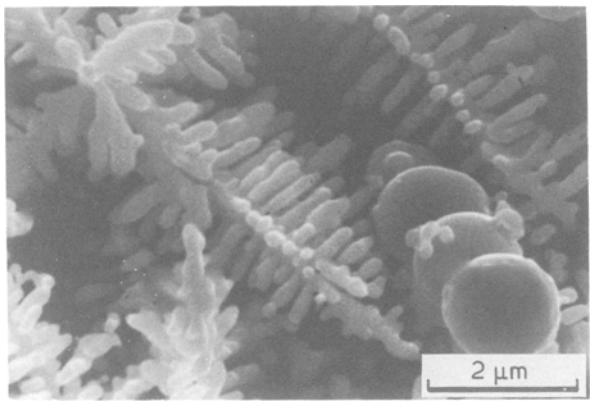


*Figure 5* Niobium microstructure after deep etching copper away. Location is point X of Fig. 3.

## 4. Discussion

The data on ingots A and B give fairly strong evidence that the ultimate tensile strength decreases with the initial dendrite diameter as $t_0^{-0.5}$. However, there is some reason to suspect that the $t_0^{-0.5}$ dependence may not be generally correct. For both ingots A and B the niobium filament spacing was measured at low $\eta$ on optical images and at high $\eta$ on SEM images taken in the BSE mode using standard stereographic intercept techniques. This approach should give a true average spacing over all niobium filaments which are imaged. Niobium filaments which are quite small, less than

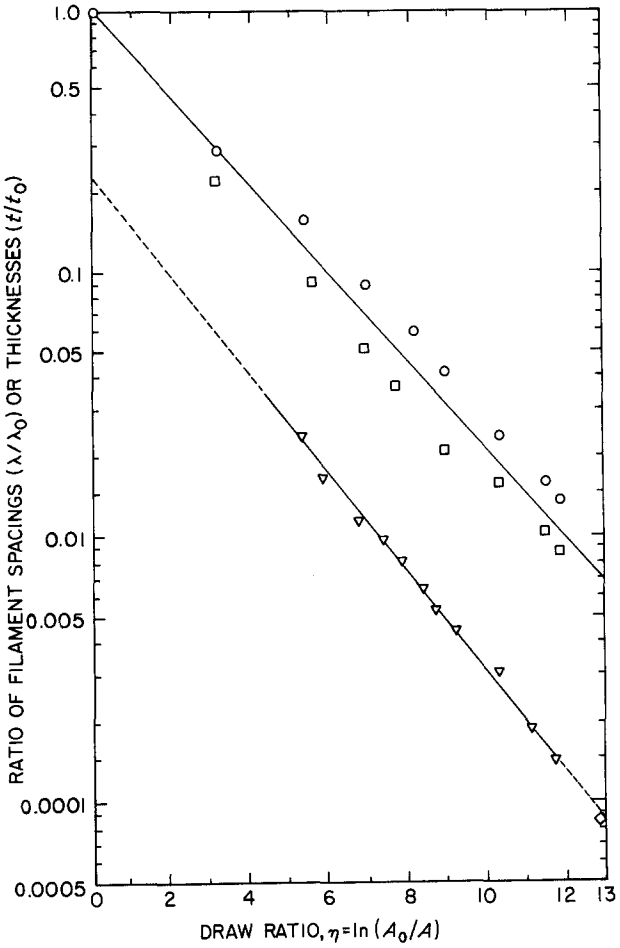


*Figure 6* Data on spacing or thickness of niobium filaments plotted against draw ratio, $\eta$. (□) $t_0 = 3.8\,\mu$m, ingot B; (○) $t_0 = 6.2\,\mu$m, ingot A; (▽) $t_0 = 8.2\,\mu$m, deep etched; (◇) $t_0 = 1.0\,\mu$m, plotted at equivalent $\eta = 12.9$.

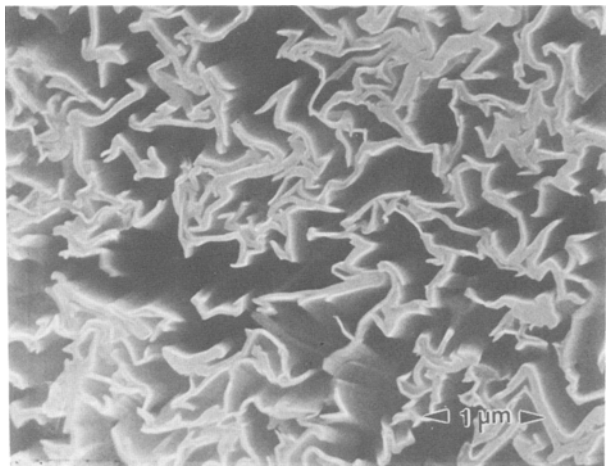


*Figure 7* Transverse section of deep-etched wire drawn to $\eta = 9.2$. Cu–20 wt % Nb.

~ 50 nm, will not be detected in the BSE images of the SEM and consequently the data will tend to overestimate the spacings and probably gives an upper bound value. The spacing data obtained for ingots A and B are given on Fig. 6 and the average line shown is fit by $t = t_0\,e^{-0.37\eta}$.

In a previous study of Cu–20 wt % alloys [14] a direct measure was made of the niobium filament thicknesses by examination of deep-etched transverse sections in a high-resolution SEM. Fig. 7 shows a typical transverse section. Several such pictures were taken at each reduction and an average filament thickness was determined by averaging over 100 filaments. The initial dendrite diameters in these ingots were quite uniform with an average value of $8.2 \pm 1.3\,\mu$m and a plot of $t/t_0$ against $\eta$ is shown as the lower curve of Fig. 6. It may be seen in Fig. 7 that there are a few filaments which appear thicker than the rest. These may have been either truly larger filaments or clusters of smaller filaments which were stuck together during the deep etch process of preparation. These larger filaments were generally avoided in the averaging, and hence the filament thicknesses measured by this technique represent a lower bound on the average value. It is clear that the thickness data taken by the deep-etch technique cannot be described by an equation of the form of Equation 2. It is physically necessary that the value of $t/t_0$ becomes 1 at $\eta = 0$, which means that the linear curve on Fig. 6 must bend upwards to $t/t_0 = 1$ at some value below $\eta \simeq 5$. Fig. 8 illustrates the appearance of the filaments in transverse section for the lowest $\eta$ studied, 5.3. It is evident that at this lowest value of $\eta$ the vast majority of filaments have already changed their distribution and morphology from the randomly arranged as-cast circular dendrites to aligned ribbons with thickness much thinner than their width. (The cause of this geometry change is well understood [15].) Continued increase in $\eta$ simply refines the filament spacing and width and the log $t$ against $\eta$ curve is linear above $\eta = 5$ as shown in Fig. 6. These data fit the equation

$$t = 1.71\,e^{-0.421\eta}\,(\mu\text{m}) \qquad (6)$$

At $\eta = 0$ the equation extrapolates to $t_0 = 1.7\,\mu$m

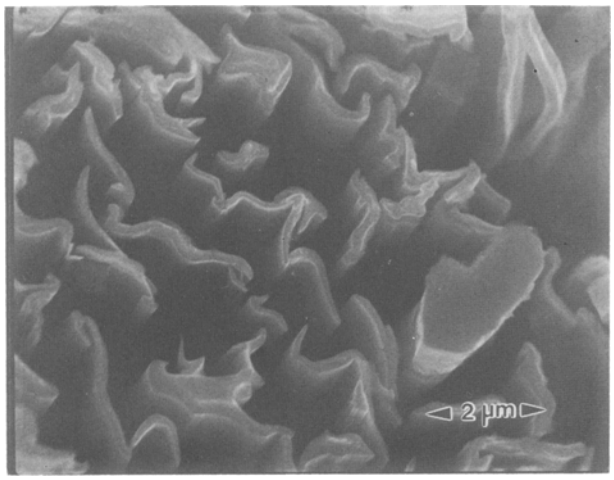


*Figure 8* Transverse section of deep-etched wire drawn to minimum $\eta$ of 5.3.

which is well below the measured $t_0$ of 8.2 $\mu$m, and clearly shows that the linear relation between ln $t$ and $\eta$ only holds at high $\eta$ values. At low $\eta$ values a dramatic change in filament morphology and distribution occurs and it is possible that this change is responsible for the required upward curvature of the data which must occur at low $\eta$ values.

The spacing data for ingots A and B of Fig. 6 extrapolate back to $\lambda/\lambda_0 = 1$ at $\eta = 0$ fairly well. Stereology considerations require the mean value of $\lambda/t$ to be a constant for constant volume fraction of niobium filaments independent of the niobium shape [16]. Because $\lambda/\lambda_0$ extrapolate to 1 at $\eta = 0$ the thickness ratio $t/t_0$ should also extrapolate to 1. The direct measurements of $t/t_0$ on the deep-etched samples shown at the bottom of Fig. 6 do not extrapolate back to 1 at $\eta = 0$ as would be expected from the $\lambda$ data. The cause of this apparent discrepancy is uncertain. Perhaps it arises because the deep-etched measurements do not measure a true mean value because of the bias in avoiding large particles in the averaging. It is our opinion that the high strength of the Cu–Nb alloys results mainly from resistance to plastic flow at the Cu–Nb interfaces. Hence, it may be that the deep-etched data are more meaningful because they weight the finer spacing more heavily, whereas the ingot A and B data weight the larger sizes more heavily. It seems reasonable, therefore, to use the data of Equation 6 to estimate the dependence of $\sigma$ upon $t_0$. Previous experiments on 12 mm diameter chill-cast Nb–20 wt % Cu alloys obtained uniform dendrite sizes of 1 $\mu$m and when reduced to $\eta = 8.7$ were found to have a filament thickness of 7 nm when measured by the deep-etch technique [17]. Equation 6 can be rewritten as $t = 1.71\ (R)^{-0.421}$, where $R = A_0/A$. The equation was obtained with ingots having $t_0 = 8.2\ \mu$m. The $t_0$ value of 1 $\mu$m in the chill castings will clearly give smaller $t$ values than predicted by the equation. If the curve for $t$ vs. $R$ for the 1 $\mu$m data where parallel to that for the 8.2 $\mu$m data then the 1 $\mu$m curve would just be shifted to higher $R$ values. It seems reasonable to assume that the higher $R$ values could be approximated by multiplying the actual $R$ values for the 1 $\mu$m ingots by the area ratio of the original dendrite sizes, $(8.2/1)^2$. Using this value for the 1 $\mu$m data the equivalent $\eta$ value (where $R = e^{\eta}$) becomes 12.9, and the data point for the 1 $\mu$m sample is seen to fall on the linear extrapolation of the curve in Fig. 6. Hence this suggests that the relation for $t$ against $\eta$ and $t_0$, after deformations large enough to establish the linear relationship, would be given as

$$\begin{aligned} t &= 1.71 \times [(8.2/t_0)^2\ e^{\eta}]^{-0.421} \\ t &= 0.291\ t_0^{0.842}\ e^{-0.421\eta} \end{aligned} \tag{7}$$

In order to use this equation with the strength data of Fig. 1, a $t_0$ of 3.8 $\mu$m is substituted into Equation 7 to obtain $t = 0.896\ e^{-0.421\eta}$. The $\sigma$ against $\eta$ data for the 3.8 $\mu$m ingot B shown in Fig. 1 fit the equation, $\sigma = 265\ e^{0.179\eta}$. Combining these latter two relations gives $\sigma = 253t^{-0.425}$ and substituting Equation 7 the following relationship is obtained

$$\sigma = 428 t_0^{-0.36}\ e^{0.179\eta} \tag{8}$$

which would only be expected to hold for large values of $\eta$ where the ln $t$ against $\eta$ curve has become linear. If this same analysis is done for the data of ingot A, $t_0 = 6.2\ \mu$m, the $t_0$ dependence is found to be $t_0^{-0.32}$. Hence, it is clear that utilizing the data on $t$ obtained by the deep etching technique in the manner described here leads to a significantly smaller dependence of $\sigma$ upon initial dendrite size than that suggested from the spacing data. Additional experiments are needed to evaluate the proper dependence.

Regardless of which relationship is more correct, Equation 8 or Equation 5, they both show that significant improvements in strength can be achieved by reducing the as-cast dendrite size, $t_0$. The data for the splat-cooled drops can be used to estimate an optimum processing design. In such a process the Cu–Nb alloy could be solidified by atomization techniques [18] thereby producing powders with very fine niobium dendrites which would then be consolidated and reduced to wire or sheet. It is seen from Figs 4 and 5 that at the high cooling rates achieved in the centre of the splat a mixed microstructure of dendrites plus spheres is obtained. This effect has been previously noted [19] and attributed to the onset of a metastable monotectic reaction which occurs in Cu–Nb alloys at high solidification rates. In the 1 $\mu$m dendrite chill castings [17] the spheres were not present. This means that the minimum dendrite size obtainable is less than 1 $\mu$m. The previous study [19] showed that the onset of the monotectic reaction is enhanced by increasing oxygen content in the molten Cu–Nb alloy. The data of Fig. 5 indicate that with proper oxygen control it may be possible to achieve niobium dendrites having $t_0$ as small as $\sim 0.3\ \mu$m. By proper classification of powder sizes in an atomization process it then might be possible to obtain powder-compacted ingots with $t_0 = 0.3\ \mu$m. Such a material would offer great improvement over the consumable arc cast material used here and having $t_0 = 3.8\ \mu$m. Going back to the example given in Section 1, to achieve a strength of 1400 MPa in the ingot B material, $t_0 = 3.8\ \mu$m, the data of Fig. 1 indicate an $\eta = 9.3$ is required. To achieve this strength in a 3 mm (1/8 in.) rod would require a starting ingot of 31 cm ($\sim$ 12 in.). If Equation 5 is correct then going to a void-free powder

processed ingot with $t_0 = 0.3\,\mu m$ would require an initial ingot diameter of only 1.1 cm, and if Equation 8 applies, the diameter would be 2.4 cm. In either case it is apparent that producing fine dendritic Cu–Nb alloys by such techniques as powder processing would offer great advantages for the production of large size pieces of high-strength Cu–Nb alloys. The example also illustrates that it is important to evaluate the correct $t_0$ dependence of $\sigma$, and future experiments are planned to evaluate this problem.

The conventional consumable arc casting of the Cu–Nb ingots offers some practical advantages over the less proven practices of powder processing on such a reactive material as Cu–Nb, which is subject to problems from oxygen contamination. It would be desirable if the as-cast niobium dendrite size in the consumable arc-casting process could be further reduced over that achieved here by removing the graphite liner. It may be possible to achieve additional size reduction by introducing electromagnetic stirring into the liquid during the freezing process.

## 5. Conclusions

1. It has been demonstrated that Cu–Nb alloys can be cast in unlined water-cooled copper moulds and that reduced niobium dendrite sizes are achieved.

2. It has been shown that it is possible to obtain as-cast niobium dendrites as small as 0.22 $\mu m$ in rapidly cooled Cu–Nb alloys.

3. It has been shown that the strength of heavily drawn Cu–Nb alloys increases significantly with reduced as-cast niobium dendrite size, $t_0$. Analysis of available data shows that the strength dependence of $\sigma$ upon $t_0$ lies somewhere between $t_0^{-0.36}$ and $t_0^{-0.5}$, but additional experiments are needed to pin down the correct dependence.

4. It has been illustrated that powder processing is an attractive process for producing high-strength Cu–Nb alloys because of its potential for achieving minimum niobium dendrite sizes.

## Acknowledgement

This work was supported by the Office of Basic Energy Sciences, Division of Materials Sciences, US Department of Energy, and it was performed at the Ames Laboratory which is operated for the US Department of Energy by Iowa University under contract no. W-7405-ENG-82.

## References

1. J. BEVK, J. P. HARBISON and J. L. BELL, *J. Appl. Phys.* **49** (1979) 6031.
2. K. R. KARASEK and J. BEVK, *Scripta Metall.* **14** (1980) 431.
3. *Idem, J. Appl. Phys.* **52** (1981) 1370.
4. P. D. FUNKENBUSCH and T. H. COURTNEY, *Acta Metall.* **33** (1985) 913.
5. P. D. FUNKENBUSCH, J. K. LEE and T. H. COURTNEY, *Met. Trans.* **18A** (1987) 1249.
6. A. R. PELTON, F. C. LAABS, W. A. SPITZIG and C. C. CHENG, *Ultramicroscopy* **22** (1987) 251.
7. S. CHUMBLEY and C. TRYBUS, unpublished research, Ames Laboratory, Ames, Iowa (1988).
8. W. A. SPITZIG, A. R. PELTON and F. C. LAABS, *Acta Metall.* **35** (1987) 2427.
9. W. A. SPITZIG and C. L. TRYBUS, unpublished research, Ames Laboratory, Ames, Iowa (1988).
10. W. A. SPITZIG and P. D. KROTZ, *Acta Metall.* (1987).
11. C. V. RENAUD, E. GREGORY and J. WONG, *Adv. Cry. Eng.* **32** (1986) 443.
12. J. D. VERHOEVEN, F. A. SCHMIDT, E. D. GIBSON and W. A. SPITZIG, *J. Metals* **38**(9) (1986) 20.
13. W. A. SPITZIG and P. D. KROTZ, *Scripta Metall.* **21** (1987) 1143.
14. J. J. SUE, J. D. VERHOEVEN, E. D. GIBSON, J. E. OSTENSON and D. K. FINNEMORE, *Acta Metall.* **29** (1981) 1791.
15. J. P. HARBISON and J. BEVK, *J. Appl. Phys.* **48** (1978) 5180.
16. E. R. UNDERWOOD, "Quantitative Stereology" (Addison-Wesley, Reading, Massachusetts, 1970) p. 83.
17. J. D. VERHOEVEN, J. J. SUE, D. K. FINNEMORE, E. D. GIBSON and J. E. OSTENSON, *J. Mater. Sci.* **15** (1980) 1907.
18. E. KLAR and J. W. FESKO, "Metals Handbook", Vol. 7, Powder Metallurgy, 9th Edn (American Society for Metals, Metals Park, Ohio, 1984) p. 25.
19. J. D. VERHOEVEN and E. D. GIBSON, *J. Mater. Sci.* **13** (1978) 1576.

*Received 23 February*
*and accepted 13 July 1988*